A Multi-wavelength analysis of M81: insight on the Arp's loop nature

A. Sollima[1], A. Gil de Paz[2], D. Martinez-Delgado[1,3], R. J. Gabany[4], J. Gallego[5], and T. Hallas[6]

[1] Instituto de Astrofisica de Canarias, La Laguna, E38205, Spain
e-mail: asollima@iac.es (AS)

[2] Departamento de Astrofisica, Universidad Complutense de Madrid, E28040, Spain

[3] Max-Planck-Institut fur Astronomie, Heidelberg, Germany

[4] Blackbird Observatory, New Mexico, USA

[5] Fosca Nit Observatory, Monsec Astronomical Park Observatory, Ager, Spain
[6] Hallas Observatory Annex, Foresthill, USA

Received January 18, 2010; accepted March 16, 2010

ABSTRACT

Context. The optical ring like structure detected by Arp (1965) around M81 (the so-called "Arp's loop") represents one of the most spectacular feature observed in nearby galaxies. Arp's loop is commonly interpreted as a tail resulting from the tidal interaction between M81 and M82. However, since its discovery the nature of this feature remains controversial.
Aims. Our primary purpose was to identify the sources of optical and infrared emission observed in Arp's loop.
Methods. The morphology of the Arp's loop has been investigated by means of deep wide-field optical images. Using IRAS and Spitzer-MIPS infrared images we measured the colors of the Arp's loop and compared them with those of the disk of M81 and dust cirrus surrounding M81.
Results. Optical images reveal that this peculiar object has a filamentary structure characterized by many dust features overlapping the field of view of M81. The ratios of far-infrared fluxes, as well as the estimated dust-to-gas ratios, indicate the infrared emission of Arp's loop is dominated by the contribution of cold dust, likely from Galactic cirrus.
Conclusions. The above results suggest that the light observed at optical wavelengths is a combination of emission from i) a few recent star formation regions located close to M81, where both bright UV complexes and peaks in the HI distribution are found, ii) the extended disk of M81 and iii) scattered light from the same Galactic cirrus that is responsible for the bulk of the far infrared emission.

Key words. Methods: data analysis – Techniques: photometric – galaxies:individual: M81 – infrared: galaxies

1. Introduction

The nearby galaxy M81 (NGC3031) together with the galaxies M82, NGC3077 and NGC2976 forms one of the most representative group of interacting galaxies. Located at a distance of $\sim$ 3.7 Mpc (Makarova et al. 2002), the M81 group has been a subject for many studies devoted to analyzing evidence of strong interactions among its components. The group contains remnants of tidal bridges connecting the three most prominent galaxies, visible in HI survey (Gottesman & Weliachew 1975; Yun et al. 1994), and over 40 dwarf galaxies (Karachentsev et al. 2001).

In particular, Arp (1965) detected an unusual ring like feature in the vicinity of M81 when examining Schmidt photographic plates. This optical feature (called "Arp's loop") is located 17 arcmin north-east of M81's center and covers a wide area ($\sim$ 160 square arcmin). It also exhibits a symmetry towards the end of the M81 disk, slightly tilted toward M82.

The Arp's loop is commonly interpreted as a tail resulting from the tidal interaction between M81 and M82. However, since its discovery the nature of this feature has been doubted by many authors. In fact, the sky region containing the M81 group of galaxies is filled by a Galactic cirrus that covers a large area of the sky near M81 (Sandage 1976). Arp's loop shares colors and emission properties similar to those observed in cirrus clouds (Abolins & Rice 1987; Appleton et al. 1993; Bremnes et al. 1998), which raised doubts about the association of this object with M81.

Subsequent analyses supporting the extra-Galactic nature of Arp's loop are based on 21cm HI observations in the M81 group region (Yun et al. 1994). These authors detected a collimated emission in the direction of the north-eastern part of the Arp's loop which blends smoothly into the structure and velocity of the HI disk of M81. Numerical simulations of the system by Yun (1999) successfully reproduced the HI tidal debris assuming M82 and NGC 3077 approached M81 during recent epochs. More recently, Makarova et al. (2002) and De Mello et al. (2008) resolved the nebular region characterized by strong HI emission into stars using deep HST observations. The analysis of their color-magnitude diagrams (CMD) shows the presence of a significant young stars population (with an age of $\sim 40-160$ Myr) and an old population characterized by a well defined Red Giant Branch. The magnitude of the tip of the Red Giant stars assumed to be associated with Arp's loop suggests a distance comparable with that of M81 (Karachentsev et al. 2002). These authors suggested that that the old component could have been removed from the M81 and/or M82 disk during their mutual interaction. Further insight have been recently provided by Barker et al. (2009) who analyzed a wide area that included M81 using deep Suprime-Cam observations. **Their results revealed no overdensity of Red Giant stars along Arp's loop extension (at odds with De Mello et al.'s results), whereas a significant group of young Red Supergiants and Main Sequence stars were evident in the confined region previously surveyed in HST studies. These authors concluded that Arp's loop was originally a gaseous tidal debris stream that formed stars only in the last 200-300 Myr. The same qualitative results have been obtained by Davidge (2009).**

In this paper we present the results of a multi-wavelength analysis of Arp's loop using the deepest optical and infrared observations available.

2. The Data

The analysis presented here is based on two datasets: *i)* a set of deep ground based optical images obtained at different facilites (the Fosca Nit Observatory and Hallas Observatories) and *ii)* a set of far-infrared images observed with MIPS at the *Spitzer Space Telescope* at 24μm, 70μm and 160μm and with IRAS using the latest IRIS data products.

The first dataset was collected with a commercially available 106mm aperture f/5 Takahashi FSQ refractor telescope of the Fosca Nit Observatory (FNO) situated near Ager (Spain) at the Monsec Astronomical Park. We used a Santa Barbara Imaging Group (SBIG) STL-11000M CCD camera which yields a large field of view ($3.9^\circ \times 2.7^\circ$) at a plate scale of 3.5 arcsec/pixel. The image set consists of multiple deep exposures through four Optec Inc. broadband (LBGR) filters. A set of individual 600 sec images were obtained during several photometric nights between January and February 2008, achieving a total exposure times of the co-added images of 17100 sec.

High resolution images were also gathered, during four photometric nights between February and March 2007, using a 14.5" f/8 RCOS cassegrain telescope situated at the Hallas Observatory Annex (HOA) situated near Foresthill (USA). A Santa Barbara Imaging Group STL-11000M camera, yielding a $41' \times 27'$ field of view and a 1 arcsec/pixel plate scale, was attached to the Cassegrain focus of the telescope. A set of images through four broadband (LGBR) filters have been secured and co-added, yielding a total exposure time of 51400 sec.

The images were reduced following standard procedures for bias correction and flat-fielding. To enhance the signal-to-noise of the faint structures around M81, image noise was attenuated with a Gaussian filter (Davis 1990).

MIPS images were also retrieved from the *Spitzer Infrared Nearby Galaxy Survey* (SINGS Data Release 4, Kennicut et al. 2003) public archive. The sample consists of a set of deep images in the 24μm, 70μm and 160μm bands. The total exposure time is approximately 220 s, 84 s and 25 s at 24μm,70μm and 160μm, respectively. Individual frames have been reduced using the MIPS Instrument Team Data Analysis Tool (Gordon et al. 2005). The background was subtracted using the average value of an empty region of the MIPS field of view. The uncertainties of the final absolute calibrations were estimated at 10% for the 24μm data and 20% for both the 70μm and 160μm data. The combined images were then aligned in the standard WCS reference frame. The overall field of view is approximately $30' \times 44'$.

To compare the colors of Arp's loop with those of nearby Galactic cirrus we also retrieved the newest generation IRIS imaging products of the IRAS sattelite covering a large region

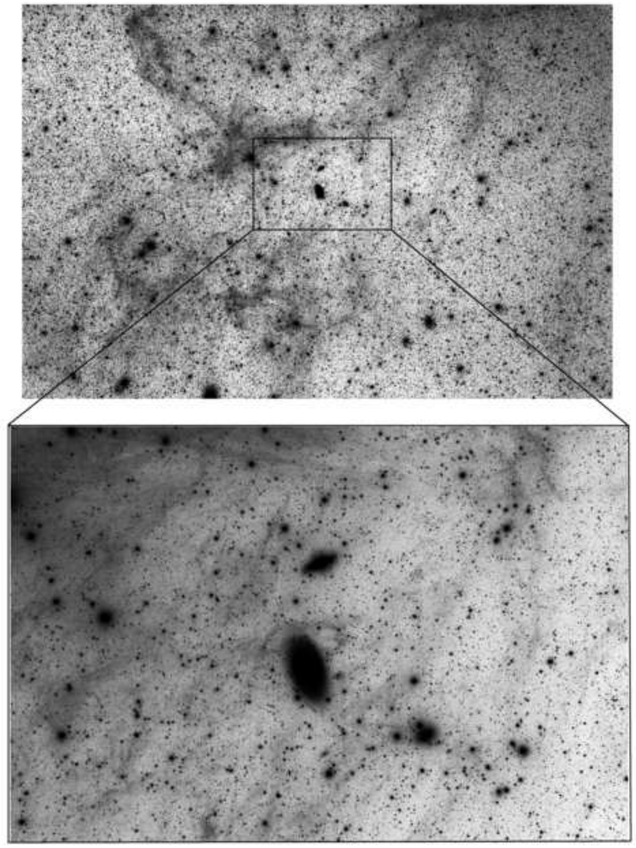

Fig. 1. Upper panel: $2^\circ \times\ 3^\circ$ image of the M81 region from Witt et al. (2008; by courtesy of S. Mandel). North is up, east to the right. Bottom panel: FNO image of the M81 group of galaxies.

($12.5^\circ \times 12.5^\circ$) around M81 (see Figure 3). The IRIS images benefit from a better zodiacal-light subtraction, calibration, zero levels, and better destriping than previous versions. In particular, the 100 μm IRIS maps represent a significant improvement over those used by Schlegel et al. (1998).

3. Results

3.1. Optical imaging

Figure 1 (low panel) shows a wide field around M81 obtained with the FNO telescope. This image clearly shows many large-scale cirrus structures. The width of these filaments range from ~ 30 arcsec up to several arcmin and extend in connective patterns over several degrees (as it is clearly visible in the panorama of this sky region displayed in the image obtained by Witt et al. 2008; see Fig.1, top panel).

Figure 2 displays the image obtained by combining all the HOA observations. This image covers an area of $41' \times 27'$. This deep image of this galaxy reaches a point-source limiting visual magnitude of $V \sim 27$. The spectacular structure of Arp's loop is evident in the north-eastern region. Arp's loop appears as a dim filamentary ring that wraps and overlaps the galaxy's disk. A careful inspection of M81's disk reveals the presence of several dust absorption features that correspond with the intersection of Arp's loop and the galaxy. These features, already noticed by Arp (1965) and Efremov et al. (1986), are due to the presence of dust in the ring, indicating that part of it should be situated between the observer and M81. In the north-eastern part of this feature (in the region where HI strong emission was found by Yun

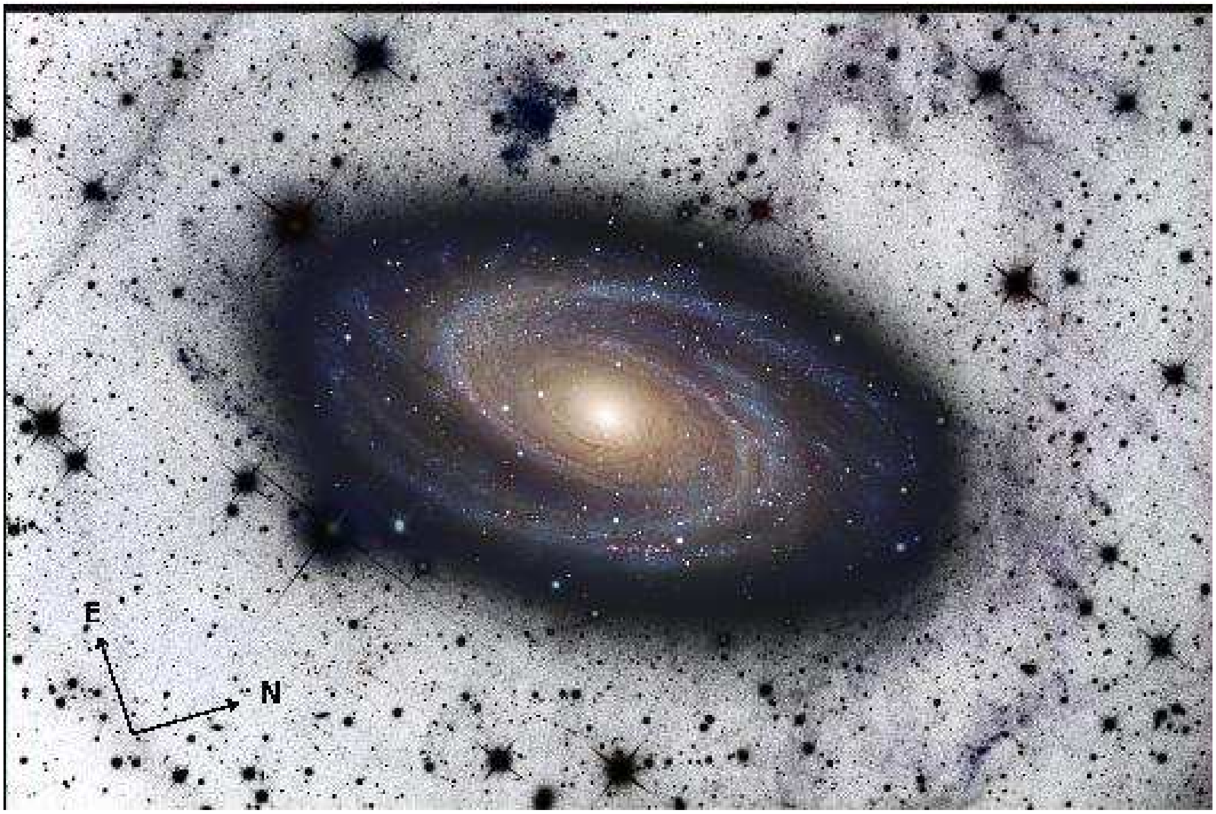

Fig. 2. Combined HOA image of the M81 region. The field of view of this image is 41′×27’. The North and east directions are indicated. Arp’s loop is visible as the nebular ring crossing the disk of M81 on the right side of the image. Dust absorbtion features are superimposed over and surround the disk of M81.

et al. 1994) a significant overdensity of stellar complexes is also apparent and suggests that new stars are still forming (Makarova et al. 2002; Mouhcine & Ibata 2010).

3.2. Far Infrared emission

As previously mentioned in Sect. 1 far infrared imaging is a fundamental tool to highlight emission from dusty objects. This is particularly important when analyzing Arp’s loop since both dust absorption in the form of dust lanes projected against the disk of M81 and dust emission from the loop itself, are clearly seen (see Sect. 3.1). The right panel of Figure 3 shows an IRAS map in a wide region (12.5° × 12.5°) around the M81 group of galaxies constructed using images in the 12μm, 60μm and 100μm bands. As noted in Figure 1, the surveyed area is filled with Galactic cirrus clouds.

To compare Arp’s loop with the cirrus clouds in infrared light, we measured the fluxes for various regions of the 60μm and 100μm IRAS image (see Figure 3). Removal of the background (mainly of cosmic origin, since zodiacal light had been previously removed from the IRIS images) was performed using the minimum value of the surface brightness in the $12.5^\circ \times 12.5^\circ$ IRIS image for each band. Despite its admittedly large amount of uncertainty, this method has been already used in the past (Carey et al. 1997) and yields a value for the background at 100 μm (0.67 MJy/sr) which is very similar to the average Cosmic Infrared Bacground of 0.78 MJy/sr as determined by Lagache et al. (2000). The selected regions, the adopted apertures and the resulting fluxes for the M81 and Arp’s loops regions are listed in Table 1.

In the left panel of Figure 3, the ratio between the 60μm and 100μm fluxes are plotted for the main body of M81 (open black point), cirrus clouds (grey points) and Arp’s loop (black filled points) as a function of the 100μm surface brightness. It should be noted that cirrus clouds occupy a well defined sequence in this diagram, with high-density cirrus showing a lower ratio than the most diffuse cirrus in the field. This trend has been previously reported by several authors (e.g. Abergel et al. 1994). For comparison, the “reference value” commonly adopted for the $I_{60\mu m}/I_{100\mu m}$ ratio in high latitude cirrus is ~ 0.2 (see e.g. Arendt et al. 1998). M81 presents a high color ($I_{60\mu m}/I_{100\mu m} \sim 0.3$) compared to Galactic cirrus of the same brightness, although it is not very different from neither diffuse cirrus colors nor from that of the loop itself. In this sense, it is worth noting that M81 is a very quiescent object in terms of its dust emission properties (see e.g. Dale et al. 2007). It has in fact the lowest $I_{60\mu m}/I_{100\mu m}$ ratio among those in the Helou (1986) sample of galaxies. More importantly, the colors found within the circular apertures placed on the loop (cyan circles in Figure 3) are not very different from the color of the M81 disk and follow the same trend as the cirrus. This latter fact suggests a Galactic origin for the bulk of the far infrared emission associated with Arp’s loop.

Despite these results, it is still conceivable that dust in the outer disk of M81, or in a potential tidal feature around M81, could show the same colors (and follow the same surface brightness trend) as the cirrus, because they could contain cold dust with emission properties similar to Galactic cirrus. The reader is referred to the recent work by Bot et al. (2009) for an extensive discussion on the properties of Galactic cirrus.

A deeper insight into the structure of dust emission around M81 necessarily requires the use of deep high-resolution

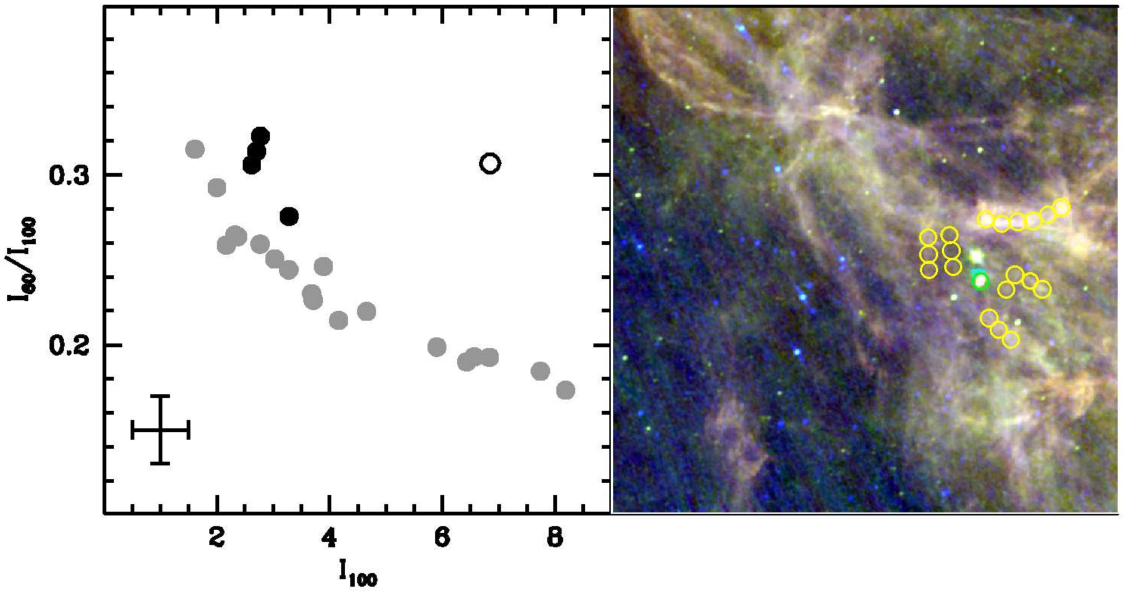

Fig. 3. In the left panel the $I_{60\mu m}/I_{100\mu m}$ ratio is shown as a function of the $I_{100\mu m}$ brightness for the loop (black filled points), M81 (open point) and the surrounding cirrus features (grey points). The typical uncertainty of the regions along Arp's loop is shown in the bottom part of the panel. The right panel depicts a false-color IRAS image of the M81 region. North is up, east is to the left. The circular apertures used in the analysis of the Galactic cirrus (yellow circles; 12' diameter), M81 (green circle; 12' diameter) and Arp's loop (tiny cyan circles above M81; 4' diameter) are shown.

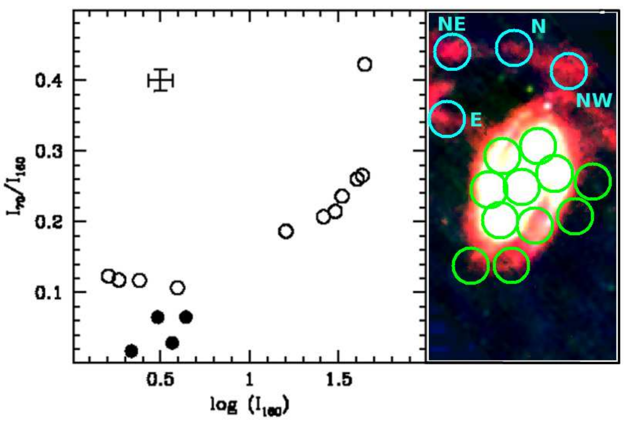

Fig. 4. In the left panel the $I_{70\mu m}/I_{160\mu m}$ ratio calculated for Arp's loop (filled circles) and the M81 disk (open circles) are shown as a function of the $I_{160\mu m}$ brightness. The typical uncertainty is shown in the upper part of the panel. In the right panel the 27′×41' color map of the Spitzer MIPS emission for M81 was constructed using the 24μm, 70μm and 160μm images. The circular apertures are also shown with the same color code used in Figure 3.

(arcmin-scale) Spitzer-MIPS observations. The MIPS 160μm data contains information at longer wavelengths that might offer further clues about the possible differences (or similarities) between dust emission in the loop and M81. The right panel of Figure 4 displays a color emission map from Spitzer. To construct this map, the MIPS/Spitzer 24μm and 70μm images were rebinned and scaled to the resolution of the 160μm image using convolution kernels developed by Gordon et al. (2008). To compare the far infrared colors of Arp's loop with the stellar component of M81 we measured the 70μm and 160μm fluxes sampled in circular apertures positioned at four regions of Arp's loop and across the M81's disk (see the right panel of Fig. 4). We exercised care in selecting both regions populated by stellar complexes and regions where only an extended diffuse emission is noticeable from optical images along Arp's loop. The measured fluxes are listed in Table 1. Most importantly, the 70μm/160μm flux ratio as a function of the 160μm brightness is shown in the left panel. Note that Arp's loop and the M81 disk displays very different colors. Here the segregation between M81 and the loop is much clearer than it is in the IRAS $I_{60\mu m}/I_{100\mu m}$ ratio. In particular, the ratio 70μm/160μm appears significantly smaller (<0.1 in all cases) than that measured on the galaxy's disk (which typically ranges between 0.2-0.4 **in the inner disk and form a plateau around 0.12 in the outer disk**) along the entire extension of the loop. The 70μm/160μm ratios measured in the loop are also similar to the 60μm/160μm ratios found by Bot et al. (2009) in their analysis of serendipitous observations contained in the Galactic cirrus of the SINGS Spitzer-MIPS fields.

3.3. Comparison between Far-Infrared and HI emission

Figure 5 displays the map of the HI emission measured by Walter et al. (2008) and the MIPS 160μm one overplotted on the optical HOA image. Notice that the HI emission nicely follows the spiral arms of M81. Also Holmberg IX (visible on the east of M81 in Figure 5) and the southtern part of Arp's loop are embedded in clouds connected to the main body of M81. On the other hand, most of the far infrared emission appears to be associated to the disk of M81, with a significant contribution from Arp's loop. In addition, note that the HI emission extends across the entire galaxy disk well beyond its optical extent, partially overlapping the Arp's loop. It is worth noting that while the 160μm flux is relatively high along the entire loop extension, the HI emission disappears in the northern part. **To better visualize this comparison, in Fig. 6 the contours of the HI emission measured by Walter et al. (2008) are overplotted to the MIPS 160μm image.** The mismatch between the spatial distribution of the HI and MIPS 160μm emission suggests that different regions of Arp's loop are characterized by different emitting mechanisms.

A more quantitative comparison has been perfomed by estimating the relative fraction of dust and gas over the Arp's loop extension and across the main body of M81. This parameter is particularly powerful in discriminating between the "canonical" emission of galactic disks and other dust-dominated sources. Indeed, this quantity span a limited range among the observed galaxies and it has been found to show a well defined radial behaviour, decreasing at large distances from the galactic center (Issa et al. 1990; Boissier et al. 2004; Munoz-Mateos et al. 2009). To estimate the total dust masses, we used MIPS fluxes at 24μm, 70μm and 160μm measured in the same circular apertures along Arp's loop and across the M81's disk defined in Sect. 3.2 (see also the right panel of Fig. 7). We adopted the relation by Munoz-Mateos et al. (2009; see their eq. A8) to convert fluxes in masses adopting a distance for M81 of 3.7 Mpc (Makarova et al. 2002). In order to obtain total gas masses we measured the HI fluxes from the M81 intensity map obtained by the THINGS survey (Walter et al. 2008). For this purpose the THINGS image has been rebinned and scaled to the resolution of the 160μm image using the convolution kernels developed by Gordon et al. (2008). The corresponding total gas masses have been calculated using eq. 3 of Walter et al. (2008). The resulting dust and HI masses together with the corresponding dust-to-gas ratios (DGR) are listed in Table 1. Equivalent radial distances from the galactic center have been therefore measured by assuming the position angle and axial ratio defined by Munoz-Mateos et al. (2009). In the left panel of Figure 7 the obtained DGR values are plotted against the equivalent angular radius along the semi-major axis. The observed profile of M81 calculated by Munoz-Mateos et al. (2009) is overplotted for comparison. As evident, at distances $r' > 200''$ the DGR shows the typical decreasing trend with galactocentric distance. Note that the DGR values measured along the Arp's loop are significantly larger than that measured in the central region of M81 deviating from the general radial trend. It is interesting to note that the maximum DGR ($log(M_{dust}/M_{gas}) \sim 0.12$) is found in the northern side of the Arp's loop, where redder MIPS colors have been measured and the HI emission drop below the detection limit. Such a large ratio has never been observed in any galaxy analysed by Munoz-Mateos et al. (2009) regardless of the distance from the galactic center. On the other hand the regions along the Arp's loop with smaller DGR values are those located in the north-eastern part of the loop (where UV complexes have been observed; De Mello et al. 2008) and in the north-western part (where the spiral arm of M81 overlaps the Arp's loop). **The surprisingly high DGR derived along the Arp's loop results from the significantly small HI fluxes measured on the Walter et al. (2008) maps. To check the dependence of the obtained results on the adopted dataset, we calculated the DGR also using the HI map provided by Yun et al. (1994). As apparent in Fig. 7, the derived DGR are very similar to those obtained using the Walter et al.'s map. Smaller intensities of the 21cm emission in the eastern and northern part of the Arp's loop are also evident in the single-dish map obtained by Appleton & van der Hulst (1988). Moreover, the HI map of Walter et al. (2008) has been constructed using VLA data decured in both C and D configurations. On the basis of all these considerations, we exclude that the large measured DGR can be addressed to problems of sensitivity and/or filtering by the interferometer of the Walter et al. (2008) data.** The large DGR measured along the Arp's loop support the idea that the far-infrared emission is increased as a result of the contribution of a dust-dominated source. In this regard, the hypothesis of the presence of a Galactic cirrus fit into this picture since it would provide a significant contribution to the far-infrared light filtering at the same time the HI emission.

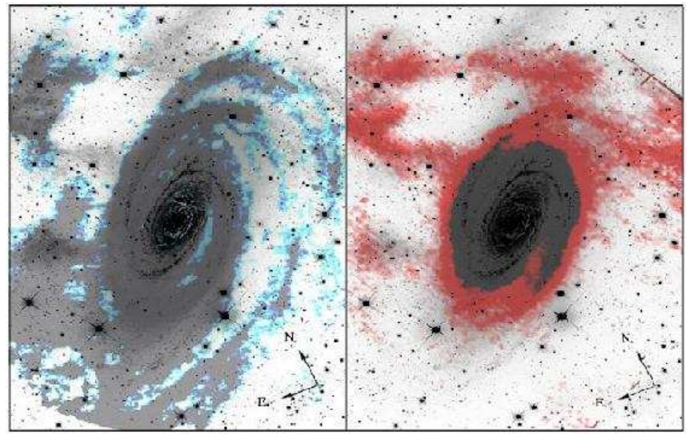

Fig. 5. HOA images of the region around M81. The HI emission from Walter et al. (2008) (left panel) and the MIPS 160ŏ3bcm image (right panel) have been overplotted.

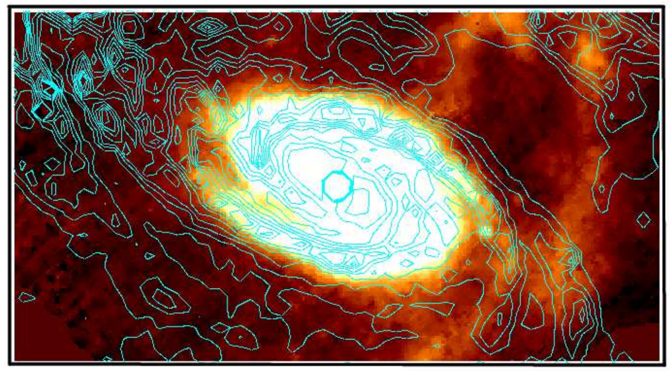

Fig. 6. MIPS 160μm image of M81. The countours of the HI emission from Walter et al. (2008) have been overplotted.

4. Discussion

This paper presents a multi-wavelength analysis of Arp's loop using the deepest optical and infrared images available.

Arp's loop appears to be formed by a filamentary wrap that partially overlaps the disk of M81. The many dust absorption features overlapping M81's field of view seen in the HOA images suggests that part of it is situated between the observer and the galaxy.

The comparison between the ratio of far infrared fluxes emitted at 70μm and 160μm by Arp's loop and M81 indicates that the emission from the loop is dominated by the contribution of cold dust. Its far infrared emission resembles the properties of Galactic cirrus clouds, which also share the same colors in the IRAS bands. The same conclusion is also supported by the analysis of the DGR measured along the Arp's loop extension which indicates a surprisingly large relative fraction of dust if compared with that expected at such a large distance from the galac-

Table 1. Far-Infrared Fluxes and dust-to-gas ratios

location	RA	Dec	diameter	$F^{IRIS}_{60\mu m}$	$F^{IRIS}_{100\mu m}$	$F^{MIPS}_{70\mu m}$	$F^{MIPS}_{160\mu m}$	M_{dust}	M_{gas}	$log\ (M_{dust}/M_{gas})$
	h m s	deg m s	$'$	Jy	Jy	Jy	Jy	$10^7\ M_\odot$	$10^7\ M_\odot$	
Arp's loop NW	09 54 34	+69 16 54	4	0.962	3.493	0.285	4.386	0.393	9.043	-1.362
Arp's loop N	09 55 43	+69 19 28	4	0.953	2.953	0.037	2.171	2.075	1.586	0.117
Arp's loop NE	09 57 02	+69 18 56	4	0.903	2.877	0.106	3.670	1.390	14.207	-1.009
Arp's loop E	09 57 09	+69 11 21	4	0.853	2.788	0.198	3.048	0.271	2.6476	-0.990
M81's disk	09 55 33	+69 03 56	12	20.101	65.550	71.98	272.300	2.520	175.790	-2.638

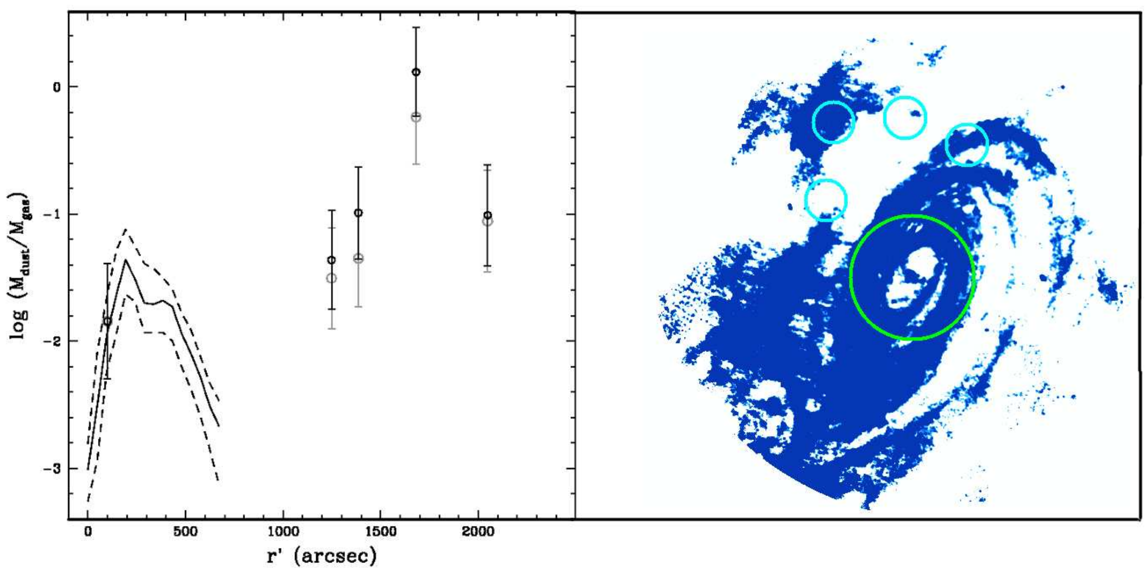

Fig. 7. In the left panel the DGR calculated for Arp's loop and the M81 disk are shown as a function of the equivalent angular distance from the galactic center. HI masses have been calculated using both Walter et al. (2008; black points) and Yun et al. (1994; grey points) HI maps. The radial DGR profile measured by Munoz-Mateos et al. (2009) is overplotted. In the right panel the THINGS image of M81 is shown. The circular apertures are also shown with the same color code used in Figure 3.

tic center. It is therefore likely that *at least part of the ring like structure that forms Arp's loop is constituted by Galactic cirrus overlaying the disk of M81*. The region around M81 is indeed known to be an area of great confusion between Galactic and extra-Galactic objects. **Of course, our observations cannot exclude the presence of a component of stripped material from the disk of M81 and/or M82 also in those regions of the Arp's loop where small $I_{70\mu m}/I_{160\mu m}$ ratios and high DGR have been measured. However, in this case a selective process in stripping preferentially dust should be at work. Hence, also in this scenario a contamination from the surrounding Galactic cirrus overlapping the Arp's loop would help to explain all the observational evidences.**

An unambiguous distinction between these two possibilities is very complex (see e.g. Cortese et al. 2010) and cannot be made solely on the basis of morphological arguments or in terms of optical colors. In fact, cirrus clouds and galaxies have largely overlapping colors (Bremnes et al. 1998) and emissions that encompass a wide range of wavelengths from the UV to the far infrared (Haikala et al. 1995).

In this context, it is important to distinguish between the stellar populations surrounding M81 and the nebular region which constitutes Arp's loop. In the last years, many sites of recent star formation have been reported in M81's outer disk by GALEX (de Mello et al. 2008). Given the wide area covered by Arp's loop, it is possible that some of these star formation regions could be located accidentally along the path of this feature. In this respect, the spatial correlation between the HI emission and the Arp's loop provides some interesting evidence. As previously mentioned in Sect. 1, these HI clouds share similar dynamics with the disk of M81. The deep photometric analyses of this region performed by Karachentsev et al. (2002), Makarova et al. (2002), Sun et al. (2005), De Mello et al. (2008), Davidge (2009) and Barker et al. (2009) revealed evidences for a young stellar population located at a distance comparable to M81. Moreover, De Mello et al. (2008) identified eight FUV sources in this region using GALEX images. The presence of a stellar component associated to M81 in this area, therefore, appears indisputable. However, notice that the HI emission disappears in the northern part of the loop where both optical and infrared images show significant contributions. Moreover, the analysis of CMDs obtained by Davidge (2009) and Barker et al. (2009) has not detected any overdensity of Red Giants along the Arp's loop and identified a population of young stars only in the confined region where the strong HI emission was observed. Thus, although the origin of part of the optical and UV emission in the Arp's loop could be emitted by recent star formation episodes, a fraction of it likely has a Galactic origin.

It is also noticeable that both HI and GALEX emissions extends across the entire disk of M81 well beyond its optical cutoff, partially overlapping the north-western part of Arp's loop (see also Gil de Paz et al. 2007; Thilker et al. 2007). This was also confirmed by the analysis of HST CMDs which revealed the presence of the M81's disk stellar population where GALEX and far infrared emissions overlap (Gogarten et al. 2009).

The observational evidence put forward in this paper suggests that the structure known as Arp's loop is likely formed by three distinct components: *i)* one associated with the M81 system that causes the emission detected in the UV and HI plus part of emission seen at optical wavelengths, thus dominating the morphology of the north-eastern part of the loop, *ii)* a second is dominated by the extended disk of M81 which contributes to the UV and HI emission in the north-western part of Arp's loop and, *iii)* another of Galactic origin that dominates the far infrared emission and is responsible for the optical morphology (through scattering by dust) of the entire ring-like structure.

Acknowledgements. This research was supported by the Instituto de Astrofísica de Canarias. We thank the anonymous referee for his/her useful comments and suggestions. We are grateful to Ignacio Trujillo, Michele Bellazzini, Julianne Dalcanton, and Juan Carlos Muñoz-Mateos for helpful discussions. We also thank Steve Mandel for providing us their wide field deep images of the M81 sky area. We also acknowledge funding from the Spanish Ministry of Education and Science (research project 2007-65090).

References

Abergel, A., Boulanger, F., Mizuno, A., & Fukui, Y., 1994, ,ApJ, 423, L59
Abolins, J. A., & Rice, W. L., 1987, NASA Conference Publication, 2466, 107
Appleton, P. N., Siqueira, P. R., & Basart, J. P., 1993, AJ, 106, 1664
Appleton, P. N., & van der Hulst, J. M., 1988, MNRAS, 234, 957
Arendt, R. G., et al., 1998, ApJ, 508, 74
Arp, H., 1965, Science, 148, 363
Barker, M.., Ferguson, A. M. ., Irwin, M., Arimoto, N., & Jablonka, P., 2009, AJ, 138, 1469
Boissier, S., Boselli, A., Buat, V., Donas, J., & Milliard, B., 2004, A&A, 424, 465
Bot, C., et al., 2009, ApJ, 695, 469
Bremnes, T., Binggeli, B., & Prugniel, P., 1998, A&AS, 129, 313
Carey, S. J., Shipman, R. F., Clark, F. O., & Assendorp, R., 1997, ApJ, 479, 303
Cortese, L., Bendo, G. J., Isaak, K. G., Davies, J. I., & Kent, B. R., MNRAS, in press, ArXiv 1001.098
Dale, D. A., et al., 2007, ApJ, 655, 863
Davidge, T. J., 2009, ApJ, 697, 1439
Davies, E. 1990, in *Machine Vision: Theory, Algorithms and Praticalities*, (Academic Press), p. 42
de Mello, D. F., et al., 2008, AJ, 135, 548
Efremov, Y. N., Karachentsev, I. D., & Karachentseva, V. E., 1986, Pis ma Astronomicheskii Zhurnal, 12, 434
Gil de Paz, A., et al., 2007, ApJS, 173, 185
Gogarten, S. M., et al., 2009, ApJ, 691, 115
Gordon, K. D., et al., 2005, PASP, 117, 503
Gordon, K. D., et al., 2008, ApJ, 682, 336
Gottesman, S. T., & Weliachew, L., 1975, ApJ, 195, 23
Haikala, L. K., et al., 1995, ApJ, 443, L33
Helou, G., 1986, ApJ, 311, L33
Issa, M. R., MacLaren, I., & Wolfendale, A. W., 1990, A&A, 236, 237
Karachentsev, I. D., Karachentseva, V. E., & Huchtmeier, W. K., 2001, A&A, 366, 428
Karachentsev, I. D., et al., 2002, A&A, 383, 125
Kennicutt, R. C., Jr., et al. 2003, PASP, 115, 928
Lagache, G., Haffner, L. M., Reynolds, R. J., & Tufte, S. L., 2000, A&A, 354, 247
Makarova, L. N., et al. 2002, A&A, 396, 473
Mouhcine, M., & Ibata, R., 2010, MNRAS, in press (arXiv:1002.0456)
Muñoz-Mateos, J. C., et al., 2009, ApJ, 701, 1965
Sandage, A., 1976, AJ, 81, 954
Schlegel, D. J., Finkbeiner, D. P., & Davis, M., 1998, ApJ, 500, 525
Sun, W.-H., et al., 2005, ApJ, 630, L133
Thilker, D. A., et al., 2007, ApJS, 173, 538
Walter, F., et al., 2008, AJ, 136, 2563
Witt, A. N., Mandel, S., Sell, P. H., Dixon, T., & Vijh, U. P., 2008, ApJ, 679, 497
Yun, M. S., 1999, in Proceedings of IAU Symposium, 186, *Galaxy Interactions at Low and High Redshift*, ed. J. E. Barnes, and D. B. Sanders, 81
Yun, M. S., Ho, P. T. P., & Lo, K. Y., 1994, Nature, 372, 530